PAR proteins regulate maintenance-phase myosin dynamics during *Caenorhabditis elegans* zygote polarization

Lawrence E. Small[a] and Adriana T. Dawes[a,b,*]
[a]Department of Molecular Genetics and [b]Department of Mathematics, The Ohio State University, Columbus, OH 43210

ABSTRACT **Establishment of anterior–posterior polarity in the *Caenorhabditis elegans* zygote requires two different processes: mechanical activity of the actin–myosin cortex and biochemical activity of partitioning-defective (PAR) proteins. Here we analyze how PARs regulate the behavior of the cortical motor protein nonmuscle myosin (NMY-2) to complement recent efforts that investigate how PARs regulate the Rho GTPase CDC-42, which in turn regulates the actin-myosin cortex. We find that PAR-3 and PAR-6 concentrate CDC-42–dependent NMY-2 in the anterior cortex, whereas PAR-2 inhibits CDC-42–dependent NMY-2 in the posterior domain by inhibiting PAR-3 and PAR-6. In addition, we find that PAR-1 and PAR-3 are necessary for inhibiting movement of NMY-2 across the cortex. PAR-1 protects NMY-2 from being moved across the cortex by forces likely originating in the cytoplasm. Meanwhile, PAR-3 stabilizes NMY-2 against PAR-2 and PAR-6 dynamics on the cortex. We find that PAR signaling fulfills two roles: localizing NMY-2 to the anterior cortex and preventing displacement of the polarized cortical actin–myosin network.**

Monitoring Editor
Denise Montell
University of California, Santa Barbara

Received: May 5, 2016
Revised: May 30, 2017
Accepted: Jun 6, 2017

INTRODUCTION

In the *Caenorhabditis elegans* zygote, generation of the anterior/posterior (A/P) axis is carried out by two cooperating processes: protein redistribution by the mechanical action of actin and myosin and biochemical activities of anterior- and posterior-specific partitioning defective (PAR) protein complexes (Kemphues *et al.*, 1988; Munro *et al.*, 2004). The proteins driving both processes function in the cortex of the embryo, where they generate distinct anterior and posterior cortical domains (Figure 1A; Etemad-Moghadam *et al.*, 1995; Guo and Kemphues, 1995; Boyd *et al.*, 1996; Tabuse, Izumi, *et al.*, 1998; Hung and Kemphues, 1999; Cuenca *et al.*, 2003; Munro *et al.*, 2004; Motegi and Sugimoto, 2006; Schonegg and Hyman, 2006). These cortical domains then direct the segregation of cytoplasmic cell fate determinants into anterior and posterior daughter cells, thus dictating the axis of the developing worm (Kemphues *et al.*, 1988; Schubert *et al.*, 2000).

The first polarizing process—mechanical action of the actin-myosin cortex—moves cortical material toward the anterior pole of the embryo (Munro *et al.*, 2004). Initially, large contractile aggregates of nonmuscle myosin II heavy chain (NMY-2) flow toward the anterior pole, leaving a relatively inactive cortical domain at the posterior pole (Figure 1A, left). This period of active polarization is known as the establishment phase (Cuenca *et al.*, 2003; Munro *et al.*, 2004).

Once the actin-myosin network has been drawn approximately halfway across the embryo, it transitions from the establishment to the maintenance phase. There is a loss of actin-myosin contraction, and the large actin-myosin aggregates are replaced by numerous smaller actin-myosin foci concentrated in the anterior domain of the embryo (Figure 1, A, middle, and B, wild type; Munro *et al.*, 2004; Motegi and Sugimoto, 2006; Schonegg and Hyman, 2006; Willis *et al.*, 2006). The extent of the embryo occupied by the actin-myosin cortex also remains relatively constant. The exact mechanism that maintains this A/P border is unknown, although it appears to require PAR protein activity (Munro *et al.*, 2004; Velarde *et al.*, 2007). This polarized morphology is maintained until cytokinesis, at which

This article was published online ahead of print in MBoC in Press (http://www.molbiolcell.org/cgi/doi/10.1091/mbc.E16-04-0263) on June 14, 2017.
The authors declare no competing financial interests.
*Address correspondence to: Adriana T. Dawes (dawes.33@osu.edu).
Abbreviations used: A/P, anterior/posterior; GFP, green fluorescent protein; NMY-2, nonmuscle myosin II heavy chain; PAR, partitioning defective; PAR-A, anterior PAR complex (PAR-3 and PAR-6, with PKC-3); PAR-P, posterior PAR complex (PAR-1 and PAR-2); RNAi, RNA interference.

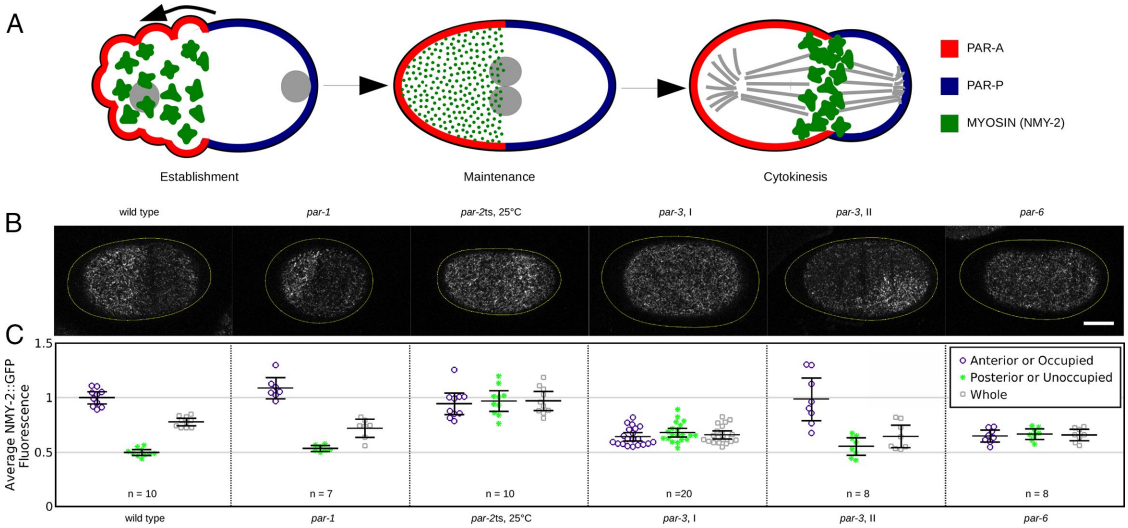

FIGURE 1: PAR-2, PAR-3, and PAR-6 are necessary during maintenance phase for proper NMY-2::GFP cortical distribution. (A) Polarization process in *C. elegans* zygotes, illustrating anterior PAR proteins (red), posterior PAR proteins (blue), and the actin-myosin network (green). In this and all subsequent figures, unless otherwise noted, the anterior pole is oriented to the left. (B) Confocal fluorescence microscopy of NMY-2::GFP on the cortex of wild-type and *par* mutant embryos during maintenance phase. *par-3*, I and *par-3*, II indicate phenotypic class I and class II *par-3* embryos, respectively (see the text for definitions). In this and subsequent figures, unless otherwise noted, images are maximum intensity projections of one side of the cortex, yellow outlines indicate the extent of the egg shell, and scale bar is 10 µm. Embryos similar to those shown here and in D are displayed in Supplemental Videos S1 (wt), S2 (*par-3*, II), S3 and S4 (*par-2*ts), and S6 and S7 (*par-1*). (C) Average NMY-2::GFP fluorescence in the anterior and posterior regions and the whole cortex of embryos represented in B. Anterior or Occupied indicates regions of visibly high NMY-2::GFP occupancy in wt, *par-1*, and *par-3* class II embryos or the anterior half of *par-2*ts, *par-3* class I, and *par-6* embryos. Posterior or Unoccupied indicates regions of visibly low NMY-2::GFP occupancy in wt, *par-1*, and *par-3* class II embryos or the posterior half of *par-2*ts, *par-3* class I, and *par-6* embryos. In this and subsequent figures, error bars indicate 95% confidence interval of the mean.

point, the cortex reassembles into the cytokinetic ring (Figure 1A, right; Willis *et al.*, 2006; Velarde *et al.*, 2007).

During the maintenance phase, NMY-2 is regulated by the Rho GTPase CDC-42. In the absence of CDC-42, NMY-2::green fluorescent protein (GFP) disappears from the anterior cortex at the establishment-to-maintenance transition (Motegi and Sugimoto, 2006; Schonegg and Hyman, 2006). Active CDC-42, bound to GTP, is localized to the anterior of the embryo (Aceto *et al.*, 2006; Kumfer *et al.*, 2010). CDC-42 is inactivated in the posterior by the regulated hydrolysis of GTP to GDP (Kumfer *et al.*, 2010). Inactive CDC-42 is reactivated in the anterior by the exchange of GDP for GTP (Kumfer *et al.*, 2010). In this way, CDC-42 activity is localized to the anterior to ultimately regulate NMY-2 localization and activity.

The second regulatory network that specifies the A/P axis is biochemical in nature and involves the PAR proteins. The PARs are a functionally diverse family of proteins that are necessary for proper specification of the zygote A/P axis and the partitioning of cytoplasmic cell fate determinants into the two daughter cells (Kemphues *et al.*, 1988; Levitan *et al.*, 1994; Etemad-Moghadam *et al.*, 1995; Guo and Kemphues, 1995; Watts *et al.*, 1996; Hung and Kemphues, 1999; Schubert *et al.*, 2000). The PAR proteins considered in this study (PAR-1, PAR-2, PAR-3, and PAR-6) localize to the cortex of the zygote, although their specific localization patterns differ (Figure 1A; Etemad-Moghadam *et al.*, 1995; Guo and Kemphues, 1995; Boyd *et al.*, 1996; Tabuse, Izumi, *et al.*, 1998; Hung and Kemphues, 1999; Motegi *et al.*, 2011). PAR-3, PAR-6, and atypical protein kinase c (PKC-3) form the anterior PAR complex (PAR-A), which localizes to the anterior pole of the zygote. PAR-1 and PAR-2 form the posterior PAR complex (PAR-P), which localizes to the posterior pole. PAR-A and PAR-P are mutually inhibitory; members of each complex are necessary to exclude the other complex from the cortex (Etemad-Moghadam *et al.*, 1995; Guo and Kemphues, 1995; Boyd *et al.*, 1996; Tabuse, Izumi, *et al.*, 1998; Hung and Kemphues, 1999; Hao *et al.*, 2006; Motegi *et al.*, 2011). It is this mutual inhibition that prevents PAR-A and PAR-P from colocalizing on the cortex, resulting in the distinct boundary between the anterior and posterior domains.

Strikingly, localization dynamics of the anterior and posterior PARs closely follows the polarization of the actin-myosin cortex during the first cell cycle (Cuenca *et al.*, 2003; Munro *et al.*, 2004). During the establishment phase, the PAR-A domain becomes restricted to the anterior, occupying the same region as NMY-2 (Figure 1A, left). As PAR-A vacates the posterior cortex, PAR-P binds to the cleared area and forms the posterior PAR domain. Actin-myosin contraction is necessary for PAR-A to completely clear the posterior of the embryo and for PAR-P to extend fully to the middle of the embryo. Similarly, PAR activity is necessary for NMY-2 to become restricted to the anterior (Munro *et al.*, 2004). The complementary localization of NMY-2 and PAR proteins and their mutual dependence show that there is a significant amount of cross-talk between the mechanical and biochemical mechanisms of polarization during the establishment phase.

PAR protein dynamics also mirror actin-myosin cortical dynamics in the maintenance phase both in localization and its dependence on CDC-42. PAR-A colocalizes with NMY-2 in the anterior domain, whereas PAR-P is restricted to the posterior domain (Figure 1A, middle; Cuenca *et al.*, 2003; Munro *et al.*, 2004). Similar to NMY-2, correct PAR protein localization requires CDC-42 (Gotta *et al.*, 2001; Kay and Hunter, 2001; Schonegg and Hyman, 2006). PAR-A requires CDC-42 for cortical association, whereas PAR-2 requires CDC-42 for

exclusion from the anterior. However, the ability of the PARs to in turn regulate actin-myosin dynamics is less characterized. It has been shown that loss of PAR-2 causes a regression of NMY-2 back into the posterior domain (Munro *et al.*, 2004). In addition, PAR-6 is necessary for proper localization of a constitutively active CDC-42 mutant (Aceto *et al.*, 2006). More recently, two studies examined specifically how activation of CDC-42 requires PAR signaling (Kumfer *et al.*, 2010; Sailer *et al.*, 2015). They found that PAR-A is required for activated CDC-42 in the anterior, whereas PAR-2 is necessary to exclude activated CDC-42 from the posterior.

The foregoing data show that there is cross-talk from the PAR pathway to the actin-myosin cortex. Indeed, some of the roles of PAR signaling in *C. elegans*, as evidenced by *par* and *nmy-2* mutant phenotypes, may be a result of cooperation between PARs and NMY-2 (Guo and Kemphues, 1996). Understanding this regulation is critical to understanding the polarization process, especially because actin-myosin and PAR proteins also work together in a number of other contexts, such as neuroblast asymmetric cell division and regulation of vesicle trafficking (Ou *et al.*, 2010; reviewed in Harris and Tepass, 2010). However, there is still not a comprehensive picture of this cross-talk. How does NMY-2 localization rely on PAR signaling? Which PAR proteins more directly regulate NMY-2? How can we uncover unexpected roles for PAR signaling in regulating cortical dynamics? To address these questions, we examined cortical NMY-2 in a variety of *par* mutant embryos, allowing us to see the effects of perturbing PAR signaling and hypothesize what elements of NMY-2 regulation remain uncharacterized. We found that PAR signaling is necessary to restrict CDC-42–dependent NMY-2 to the anterior cortex during the maintenance phase. We also found that PAR signaling prevents displacement of the polarized actin-myosin cortex.

RESULTS

par genes regulate NMY-2 association with the cortex

In the maintenance phase of the *C. elegans* zygote, NMY-2 is localized to the anterior cortex (Figure 1A; Munro *et al.*, 2004). This is the same region occupied by PAR-A proteins PAR-3 and PAR-6 (Figure 1A; Hung and Kemphues, 1999; Cuenca *et al.*, 2003). To determine whether the PAR proteins have a role in regulating NMY-2 association with the cortex, we examined localization of NMY-2::GFP in embryos of different *par* mutant backgrounds.

We first examined NMY-2::GFP localization in embryos with anterior *par* mutations: the amber mutant *par-3(e2074)* and the RNA-null *par-6(zu222)* (Kemphues *et al.*, 1988; Cheng *et al.*, 1995; Hung and Kemphues, 1999; for simplicity, here and elsewhere, embryo genotypes and RNA interference [RNAi] refer to the maternal contribution to the embryo). In *par-3* mutant embryos, we observed two phenotypes: uniform distribution of NMY-2::GFP over the entire visible cortex (20 of 28, designated as phenotype class I) or a mislocalized patch of NMY-2::GFP (8 of 28, designated as phenotype class II; Figure 1B, *par-3*, I and *par-3*, II, respectively). In *par-3* class I embryos, the total amount of NMY-2::GFP on the cortex decreased slightly relative to wild type, even as posterior NMY-2::GFP increased (Figure 1C). In *par-3* class II embryos, the patch of NMY-2::GFP moved across the cortex of the embryo (wild type, Supplemental Video S1; *par-3*, Supplemental Video S2). We conclude that *par-3* is required to properly restrict NMY-2 to the anterior cortex. In *par-6* mutant embryos, we observed uniform, intermediate levels of NMY-2::GFP, similar to *par-3* class I (Figure 1, B and C). However, we did not observe any *par-6* class II embryos (0 of 28 embryos). This difference indicates that PAR-3 and PAR-6 have distinct roles with respect to NMY-2::GFP cortical association, but both are necessary for restricting NMY-2::GFP to the anterior of the embryo.

We next examined NMY-2::GFP localization in embryos with posterior *par* mutations: the truncation mutant *par-1(b274)* and the temperature-sensitive *par-2(or373*ts*)* (Kemphues *et al.*, 1988; Hurd and Kemphues, 2003; O'Rourke *et al.*, 2011). In *par-2*ts mutant embryos at the restrictive temperature, ectopic NMY-2::GFP associated with the posterior cortex during the maintenance phase (Figure 1, B and C). In contrast, in *par-1* embryos, NMY-2::GFP was associated with the anterior cortex as in wild-type embryos, except that occasionally the domain of anterior NMY-2::GFP was reduced in size, as previously reported for actin (Figure 1, B and C; Velarde *et al.*, 2007). The anterior domain accumulated NMY-2::GFP to at least wild-type average levels, although the domain's reduced size caused the total amount of NMY-2::GFP to drop slightly. These results indicate that the posterior PAR-2, but not its posterior companion PAR-1, is necessary to exclude NMY-2::GFP from the posterior cortex.

It has been shown that PAR-2 prevents both ectopic association of NMY-2 with the posterior cortex and regression of polarized NMY-2 from the anterior domain back into the posterior domain at the transition from the establishment to the maintenance phase (Munro *et al.*, 2004). In our hands, many *par-2*ts embryos showed the regression observed by Munro *et al.* (2004), whereas others showed ectopic NMY-2::GFP association without regression (Supplemental Videos S3 and S4). It has also been shown that PAR-3 is necessary to regulate association of NMY-2::GFP with the maintenance-phase cortex in embryos lacking establishment-phase NMY-2::GFP (Zonies *et al.*, 2010). We saw an increase in NMY-2::GFP fluorescence across the cortex of *par-3* class I embryos and in the forming NMY-2::GFP patch in *par-3* class II embryos (class I, Supplemental Video S5; class II, Supplemental Video S2). Thus our observations agree with previous research showing that PAR-2 and PAR-3 are necessary to prevent de novo, ectopic NMY-2::GFP cortical association.

PAR-2 requires PAR-3 and PAR-6 to regulate NMY-2 cortical association

Distinct PAR-A and PAR-P cortical domains are maintained by the ability of each complex to remove the other from the cortex (Hao *et al.*, 2006). Because of this mutual inhibition, we sought to determine how PAR-A and PAR-P work together to regulate NMY-2 cortical association. Zonies *et al.* (2010) found in *par-3* mutant embryos, PAR-2 was no longer required to prevent ectopic, anterior-like NMY-2 in the posterior domain. However, Beatty *et al.* (2013) found that in *par-6* mutant embryos, PAR-2 was still necessary to prevent anterior-like NMY-2 in the posterior domain. In light of these seemingly contradictory results, we sought to clarify how PARs regulate the association of NMY-2 with the cortex.

When *par-3* worms were treated with *par-2* RNAi, the *par-3* mutant allele was epistatic to *par-2* RNAi, causing a significant reduction in NMY-2::GFP across the cortex of embryos treated with *par-2* RNAi (Figure 2, A and B). The exception to this epistasis is that *par-2* RNAi caused a loss of *par-3* class II mutant phenotypes (empty vector, 6 of 20; *par-2* RNAi, 0 of 29; $p < 0.01$ by Fisher's exact test). Similarly, in our hands, the *par-6* mutant allele was also epistatic to *par-2* RNAi, resulting in uniformly medium levels of NMY-2::GFP on the cortex (Figure 2, C and D). Thus we observed that both anterior PARs, *par-3* and *par-6*, are epistatic to *par-2*.

We also observed that *par-3* RNAi in *par-6* mutant embryos produced no significant difference in NMY-2::GFP association from that of either *par-6* mutant embryos treated with empty vector RNAi or *par-6*/+ balanced embryos treated with *par-3* RNAi (Figure 2, C and D), as would be expected if PAR-3 and PAR-6 require each other to function (Watts *et al.*, 1996; Hung and Kemphues, 1999).

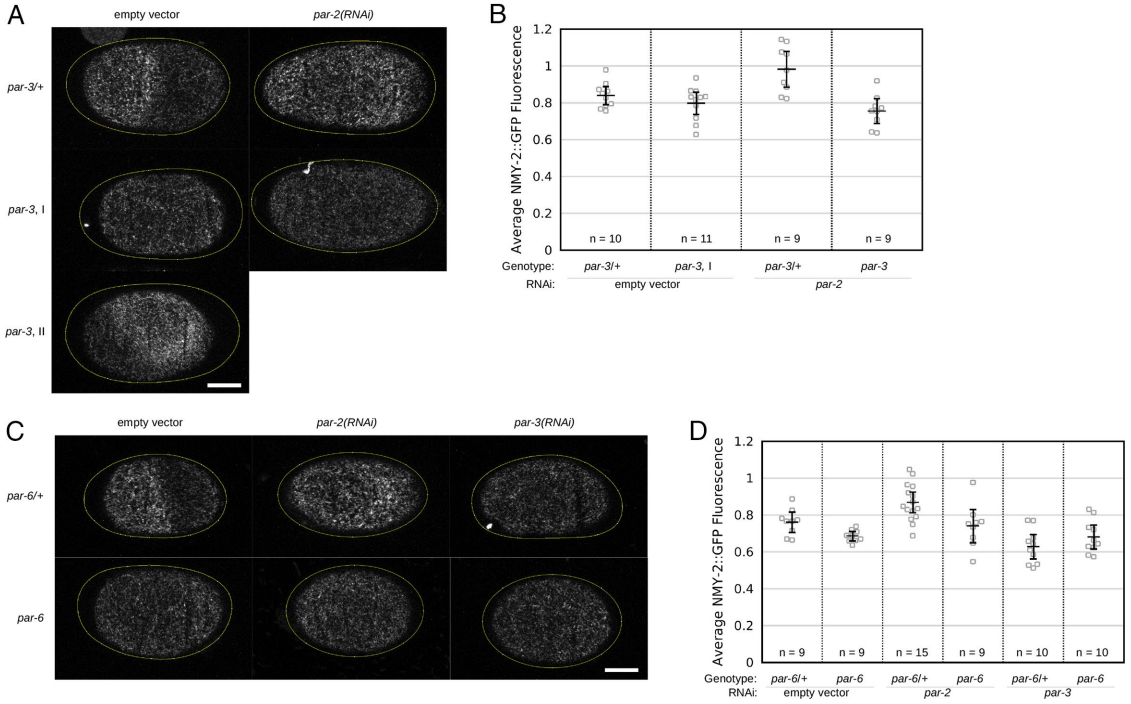

FIGURE 2: PAR-2 requires PAR-3 and PAR-6 to regulate NMY-2::GFP cortical association. Confocal fluorescence microscopy of NMY-2::GFP on the cortex of maintenance phase embryos, combining *par-3* (A, B) or *par-6* (C, D) mutations with *par-2*, *par-3*, and *par-6* RNAi. Quantification (B, D) is of average NMY-2::GFP fluorescence in the entire visible cortex of embryos represented here, normalized to average anterior NMY-2::GFP level of *par*/+, empty vector embryos.

However, RNAi against *par-3* produced no class II embryos in both *par-6* and *par-6*/+ worms, suggesting that the presence of a moving patch of NMY-2::GFP requires wild-type levels of PAR-6 and that PAR-6 is still able to influence the cortex in the absence of PAR-3. Taken together, our results indicate that, with respect to NMY-2 regulation, PAR-2 mainly functions to restrict PAR-A to the anterior of the embryo, whereas anterior PARs more directly promote the accumulation of anterior-like levels of NMY-2 (Figure 3). The anterior PARs generally require each other for NMY-2 polarization, but occasionally, in the absence of PAR-3, PAR-2 and PAR-6 are capable of supporting the formation of NMY-2 patches.

CDC-42 is necessary for NMY-2 cortical association in *par* mutant embryos

In wild-type embryos, the Rho GTPase CDC-42 is critical for recruiting high levels of NMY-2 to the anterior cortex during the maintenance phase (Motegi and Sugimoto, 2006; Schonegg and Hyman, 2006). Because *par* mutations cause aberrant NMY-2 localization, we sought to determine whether the misregulated NMY-2 described earlier was similarly dependent on CDC-42. Strong *cdc-42* RNAi completelyeliminatespolarized,anteriorNMY-2::GFP(MotegiandSugimoto, 2006; Schonegg and Hyman, 2006); therefore, we only partially reduced *cdc-42* levels in *par* mutant embryos so that NMY-2::GFP polarization was still visible (see *Materials and Methods*). When *cdc-42* was reduced in balanced embryos, NMY-2::GFP levels on the cortex were reduced by ~31% (Figure 4B). In *par-2* mutant embryos, *cdc-42* reduction lowered NMY-2::GFP levels by a similar amount (Figure 4, A and B), indicating that ectopic posterior NMY-2::GFP is still dependent on CDC-42. This suggests that PAR-2 specifically inhibits CDC-42-dependent NMY-2 in the posterior domain.

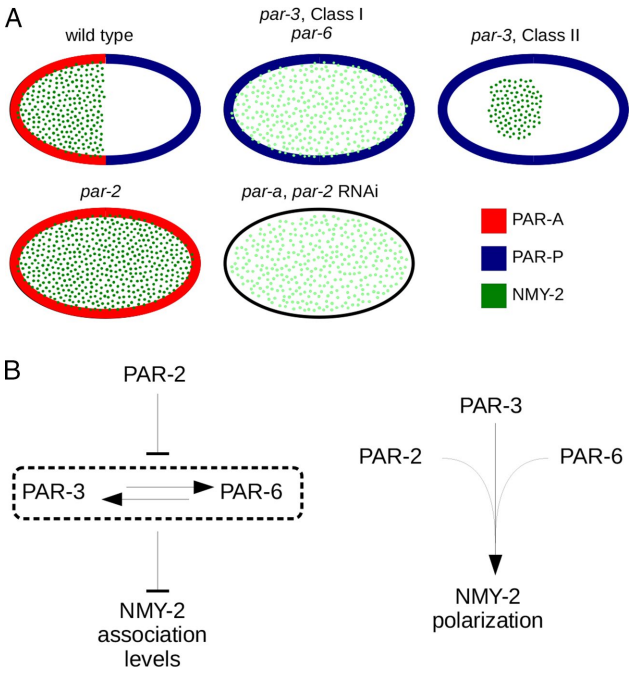

FIGURE 3: PAR proteins regulate NMY-2 association and polarization. (A) Illustration of observed NMY-2::GFP cortical associations under different combinations of *par* mutation and RNAi. PAR-A, PAR-P, and NMY-2 proteins are represented as in Figure 1A. *par-a* = *par-3* or *par-6*. (B) Cartoon of observed genetic interactions. Pointed arrows indicate positive interactions, and blunt arrows indicate negative interactions.

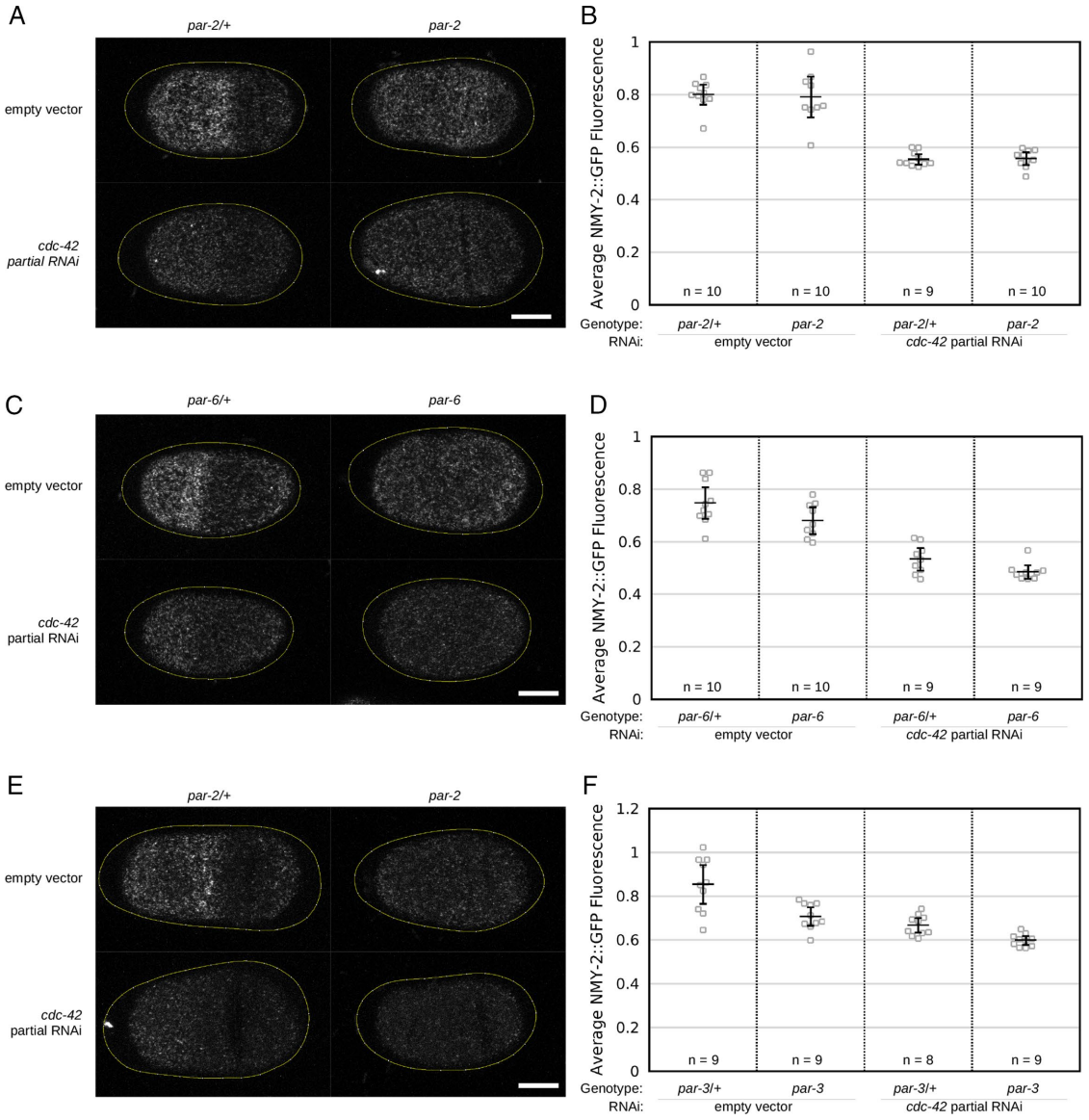

FIGURE 4: CDC-42 is necessary for NMY-2::GFP cortical association in *par* mutant embryos. Confocal fluorescence microscopy of NMY-2::GFP on the cortex of maintenance-phase embryos, combining *par-2* (A, B), *par-6* (C, D), or *par-3* (E, F) mutations with *cdc-42* partial RNAi. Quantification (B, D, F) is of average NMY-2::GFP fluorescence in the entire visible cortex of embryos represented here, normalized to average anterior NMY-2::GFP level of *par*/+, empty vector embryos.

When *cdc-42* was reduced in *par-3* or *par-6* mutant embryos, NMY-2::GFP was also reduced on the cortex (Figure 4, C and D, *par-3*; and E and F, *par-6*). This reduction was uniform across the cortex, indicating that NMY-2::GFP across the entire cortex in *par-3* and *par-6* embryos is dependent on CDC-42. Similar to *par-2*, this indicates that *par-3* and *par-6* are important in restricting specifically CDC-42–dependent NMY-2::GFP to the anterior cortex.

PAR-1 and PAR-3 suppress NMY-2 movement during maintenance phase

The mobility of the NMY-2::GFP patch observed in *par-3* class II embryos (Supplemental Video S2) prompted us to ask whether *par* genes not only regulate NMY-2 association but also suppress NMY-2 cortical movement during the maintenance phase. To assay this, we measured the movement of NMY-2::GFP foci across the cortex in wild-type and *par* mutant embryos. In wild-type embryos during the maintenance phase, NMY-2::GFP foci moved across the cortex at an average speed of ~0.02 μm/s (Figure 5, A and B), and movement generally proceeded in the posterior direction (Figure 5, A and C). The most striking phenotype was seen in *par-1* embryos, in which NMY-2::GFP foci speed increased to ~0.06 μm/s (Figure 5, A and B). In addition, in *par-1* embryos, NMY-2::GFP foci moved in the circumferential direction on average, around the A/P axis rather than toward the anterior or posterior pole of the embryo (Figure 5, A and C, and Supplemental Video S5), although occasionally we did see movement along the A/P axis (Supplemental Video S6). PAR-1 protein in wild-type embryos is localized to the posterior cortex (Etemad-Moghadam *et al.*, 1995), so we anticipated that ectopic NMY-2::GFP movement would be greatest in the posterior region. Surprisingly, NMY-2::GFP foci moved at similar speeds in both the anterior and posterior regions of the embryo, indicating that PAR-1 suppresses NMY-2::GFP movement throughout the embryo (Supplemental Figure S1 and Supplemental Video S5).

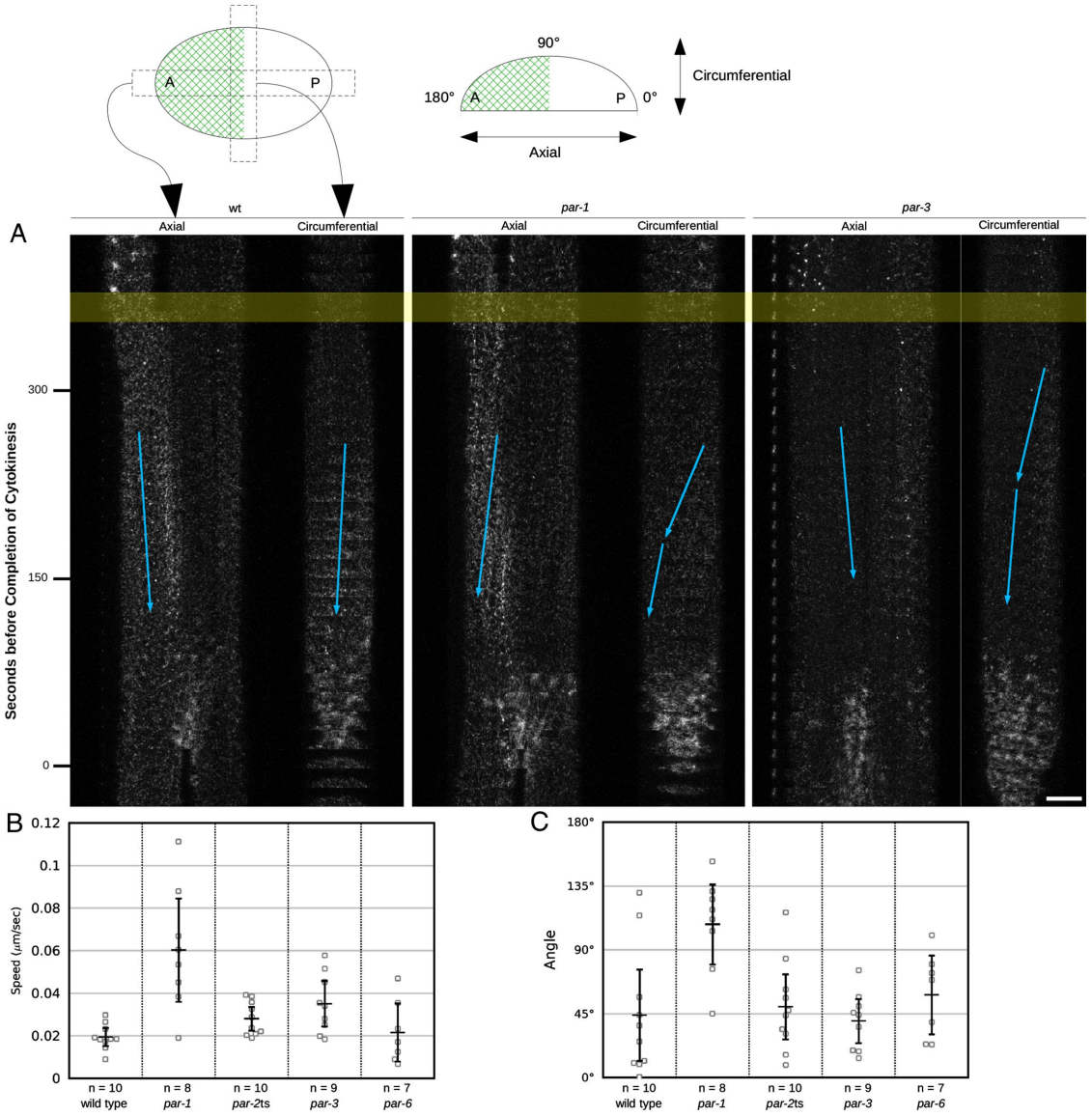

FIGURE 5: PAR-1 and PAR-3 suppress NMY-2::GFP movement during maintenance phase. (A) Movement of cortical NMY-2::GFP in wild-type and *par* mutant embryos. Here and in subsequent figures, kymographs are constructed from maximum intensity projections like those in Figure 1B. Axial and circumferential sections are described in *Materials and Methods*. Blue arrows trace the movement of NMY-2::GFP foci across the cortex through time. The yellow bar indicates the transition from establishment phase to maintenance phase. In circumferential kymographs, the anterior pole is oriented downward in each individual section. Embryos similar to those shown here are displayed in Supplemental Videos S1 (wt) and S6 (*par-1*). (B, C) Average speed (B) and direction (C) of movement of NMY-2::GFP foci in wild-type and *par*-mutant embryos. In this and subsequent figures, an angle of 0° represents movement toward the posterior pole, and an angle of 180° represents movement toward the anterior pole; no distinction is made between up or down movements orthogonal to the A/P axis.

Studies indicated that the *par-1(b274)* allele used here has neomorphic activity in the anterior cytoplasm rather than being null (Hurd and Kemphues, 2003; Tenlen *et al.*, 2008; Griffin *et al.*, 2011). To address this possibility, we performed RNAi against *par-1* in *par-1(b274)* mutant embryos, which should deplete them of any mutant PAR-1 protein. We found that not only did *par-1* RNAi not suppress our ectopic NMY-2::GFP movement phenotype, but it also replicated the *par-1(b274)* phenotype in balanced, *par-1(b274)/+* worms (Supplemental Figure S2). We therefore conclude that our particular *par-1* mutant phenotypes are not the result of the presence of a neomorphic *par-1(b274)* allele but instead are the result of loss of the wild-type *par-1* allele.

NMY-2::GFP foci were also more mobile in *par-2* and *par-3* embryos. In *par-2* embryos, we saw increased NMY-2::GFP movement (Figure 5B), which corresponded well with that reported by Munro *et al.* (2004) and Sailer *et al.* (2015). *par-3* embryos also showed increased NMY-2::GFP movement on the cortex during the maintenance phase (Figure 5, A and B), although the direction of movement was not significantly different from wild type (Figure 5, A and C). When we examined NMY-2::GFP movement through time, NMY-2::GFP speed in *par-1* embryos increased gradually as the

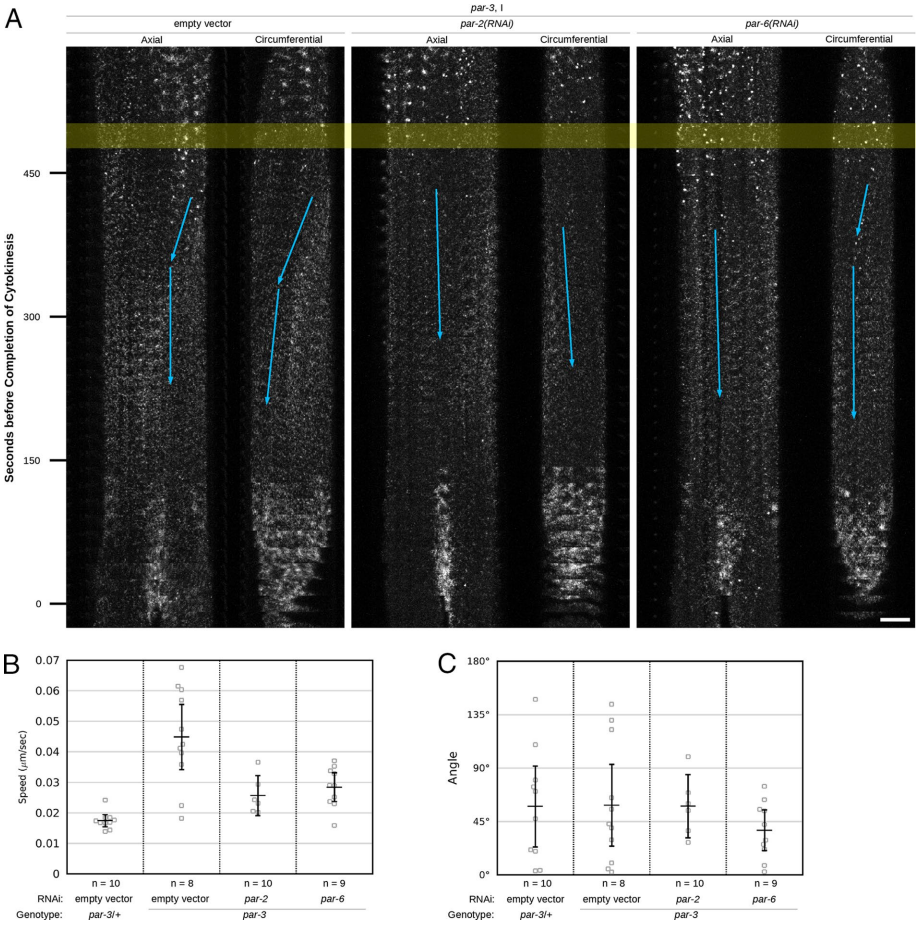

FIGURE 6: PAR-2 and PAR-6 drive NMY-2::GFP cortical movement in the absence of PAR-3. (A) Movement of cortical NMY-2::GFP in *par-3* mutant embryos treated with empty vector or par RNAi. Only class I embryos were observed when *par-2* or *par-6* RNAi was combined with *par-3* embryos (see Figure 1, C and D), so only *par-3*, empty vector class I embryos are displayed. Kymographs are constructed as in Figure 5. (B, C) Average speed (B) and direction (C) of movement of NMY-2::GFP foci in *par-3*, class I mutant and *par-3*/+ balanced embryos treated with empty vector or *par* RNAi. Graphs are constructed as in Figure 5.

maintenance phase progressed, and *par-3* embryos showed elevated NMY-2::GFP speed particularly in the middle of the maintenance phase (Supplemental Figure S3). Thus we conclude that PAR-1 and PAR-3, along with PAR-2, as previously reported, are necessary to suppress movement of the cortex during the maintenance phase.

One caveat of our method of measurement is that the entire embryo is not featured in the analyzed kymographs but instead is represented by two perpendicular kymographs "centered" on the midpoint of the embryo. To address this issue, we also measured movement by tiling kymographs across the entire visible surface of the embryo (Supplemental Figure S4A). The resulting "tiled" analysis produced trends similar to centered analysis, with two differences. Our observed *par-2* NMY-2::GFP movement phenotype disappeared in tiled analysis (Supplemental Figure S4, A and B). This is contrary to the phenotypes observed by Munro *et al.* (2004) and Sailer *et al.* (2015). The phenotype they observed manifested near the posterior pole, and so it is likely that tiled kymographs situated at the extreme top and bottom of the image, which do not touch the posterior pole, cannot contain this movement, and this suppresses the observed effect. We also saw that, with tiled analysis, the observed *par-1* NMY-2::GFP movement phenotype was present but reduced (Supplemental Figure S4, A and B). This seems anomalous because separate measurement of the anterior and posterior domains by centered analysis, as well as visual inspection of image sequences, showed that significant NMY-2::GFP foci movement occurs in both the anterior and posterior of the embryo (Supplemental Figure S1 and Supplemental Video S5). As a result of these discrepancies, we used centered analysis for the remainder of the study.

PAR-2 and PAR-6 drive NMY-2 movement in the absence of PAR-3

Given that PAR-2 and PAR-6 are necessary for *par-3* class II phenotypes (Figure 2), we tested whether they also are necessary for ectopic NMY-2 movement. In *par-3* mutant embryos treated with *par-2* RNAi, we observed that the average speed of NMY-2::GFP movement on the cortex was significantly decreased relative to empty vector RNAi (Figure 6, A and B). Similarly, *par-6* RNAi in *par-3* mutant embryos also caused a significant decrease in NMY-2::GFP speed (Figure 6, A and B). This indicates that both PAR-2 and PAR-6 are necessary for the *par-3* NMY-2::GFP movement phenotype. However, there was no significant change in the direction of NMY-2::GFP movement (Figure 6C), suggesting that the direction of movement is set by some asymmetric feature that does not rely on maintenance-phase PAR asymmetries.

PAR-2, PAR-3, and PAR-6 set the direction of PAR-1–inhibited NMY-2 movement

Given that PAR-2 and PAR-6 are required for PAR-3–inhibited movement, we hypothesized that they also drive PAR-1–inhibited movement. To test this hypothesis, we assayed NMY-2::GFP movement in *par-1* embryos depleted of *par-2*, *par-3*, and *par-6* by RNAi. We noted that NMY-2::GFP in *par-1*, *empty vector RNAi* embryos moved more slowly than in untreated *par-1* mutant embryos (contrast Figure 5 with Figures 7 and 8). This is possibly a consequence of the different culturing conditions and elevated incubation temperature of RNAi experiments (25 vs. 20°C). In addition, the variation within different *par-1* mutant embryo populations can be relatively high, likely contributing to variation between experiments. When any of *par-2*, *par-3*, or *par-6* was knocked down in *par-1* embryos, the speed of NMY-2::GFP movement was unaffected (Figure 7, A and B). However, rather than moving circumferentially around the embryo, NMY-2::GFP foci moved in a more posterior direction (Figure 7, A and C). This suggests that in the absence of PAR-1, the other PARs act to restrict NMY-2::GFP from moving back into the posterior domain. When any of *par-2*, *par-3*, or *par-6* is removed from the embryo, A/P asymmetry is lost (Figure 1B), and so NMY-2::GFP is free to move into the posterior. It is intriguing that the speed of NMY-2::GFP movement did not change when NMY-2::GFP asymmetry was lost. We conclude that, unlike PAR-3, PAR-1-inhibited movement does not emerge from dynamic interactions between anterior and posterior PARs (Figure 9, A and B).

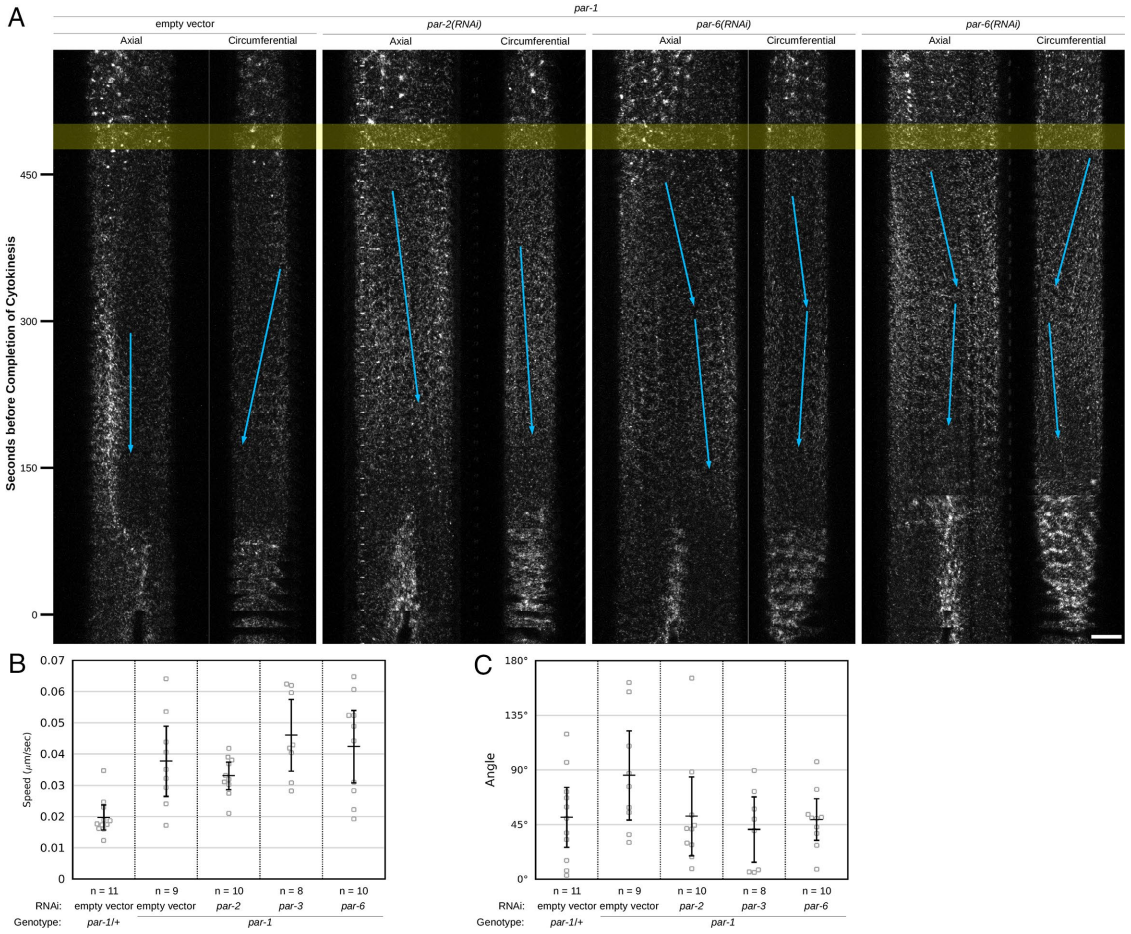

FIGURE 7: PAR-2, PAR-3, and PAR-6 set the direction of PAR-1–inhibited NMY-2::GFP movement. (A) Movement of cortical NMY-2::GFP in *par-1* mutant embryos treated with empty vector or par RNAi. Kymographs are constructed as in Figure 5. (B, C) Average speed (B) and direction (C) of movement of NMY-2::GFP foci in *par-1* mutant and *par-1/+* balanced embryos treated with empty vector or *par* RNAi. Graphs are constructed as in Figure 5.

CDC-42 inhibits NMY-2 movement in the absence of PAR-1

Because PAR-1–inhibited NMY-2::GFP ectopic movement is not driven by PAR dynamics, we hypothesized that movement requires CDC-42, which regulates the actin-myosin cortex during the maintenance phase. We reduced *cdc-42* levels by partial RNAi (see *Materials and Methods*). Unexpectedly, *cdc-42* reduction in *par-1* embryos caused NMY-2::GFP movement to increase significantly (Figure 8, A and B). The direction of movement, however, was unchanged (Figure 8, A and C). Thus CDC-42 does not drive NMY-2::GFP movement in the absence of PAR-1 but instead inhibits it (Figure 9B). Also note that movement does not strictly rely on the levels of NMY-2 on the cortex.

DISCUSSION

Cross-regulation between PAR proteins and NMY-2 on the cortex

In this study, we characterized two different roles for PAR signaling in the regulation of NMY-2 on the cortex. First, PAR signaling restricts NMY-2 cortical association during the maintenance phase to the anterior of the embryo. Second, PAR proteins prevent the displacement of polarized NMY-2 on the cortex. Together these two roles help to maintain proper NMY-2 cortical dynamics. Liu, Maduzia, *et al.* (2010) showed that NMY-2 is necessary to stabilize the polarity of the maintenance-phase cortex. In its absence, the anterior PAR-6 domain expands and the posterior PAR-2 domain retracts. Here we show that PAR proteins similarly promote proper NMY-2 association with the anterior cortex. This suggests cooperation between PAR and NMY-2 polarity. We speculate that PAR signaling polarizes NMY-2 for the purpose of stabilizing the PAR domains. A similar hypothesis was proposed for actin and PAR-3/6 by Velarde *et al.* (2007) and for NMY-2 and PAR-2 by Munro *et al.* (2004) and Motegi and Sugimoto (2006), and here we extend this idea to hypothesize that PAR-3 and PAR-6 concentrate NMY-2 in the anterior, so that the domain boundary maintains its proper position.

Mechanisms by which PAR proteins may regulate NMY-2 cortical association

The molecular mechanism by which PAR proteins regulate NMY-2 cortical association is still undetermined. One hypothesis is that PAR proteins directly regulate CDC-42 activity, which then promotes NMY-2 cortical association. Recent evidence indicated a positive physical interaction between PAR-6 and CDC-42 (Aceto *et al.*, 2006; Kumfer *et al.*, 2010; Sailer *et al.*, 2015). Of interest, our *cdc-42* partial knockdown experiments suggest that CDC-42 still has residual activity in the absence of PAR-6, which is contrary to previous observations (Kumfer *et al.*, 2010). A potential explanation is that PAR-6 is

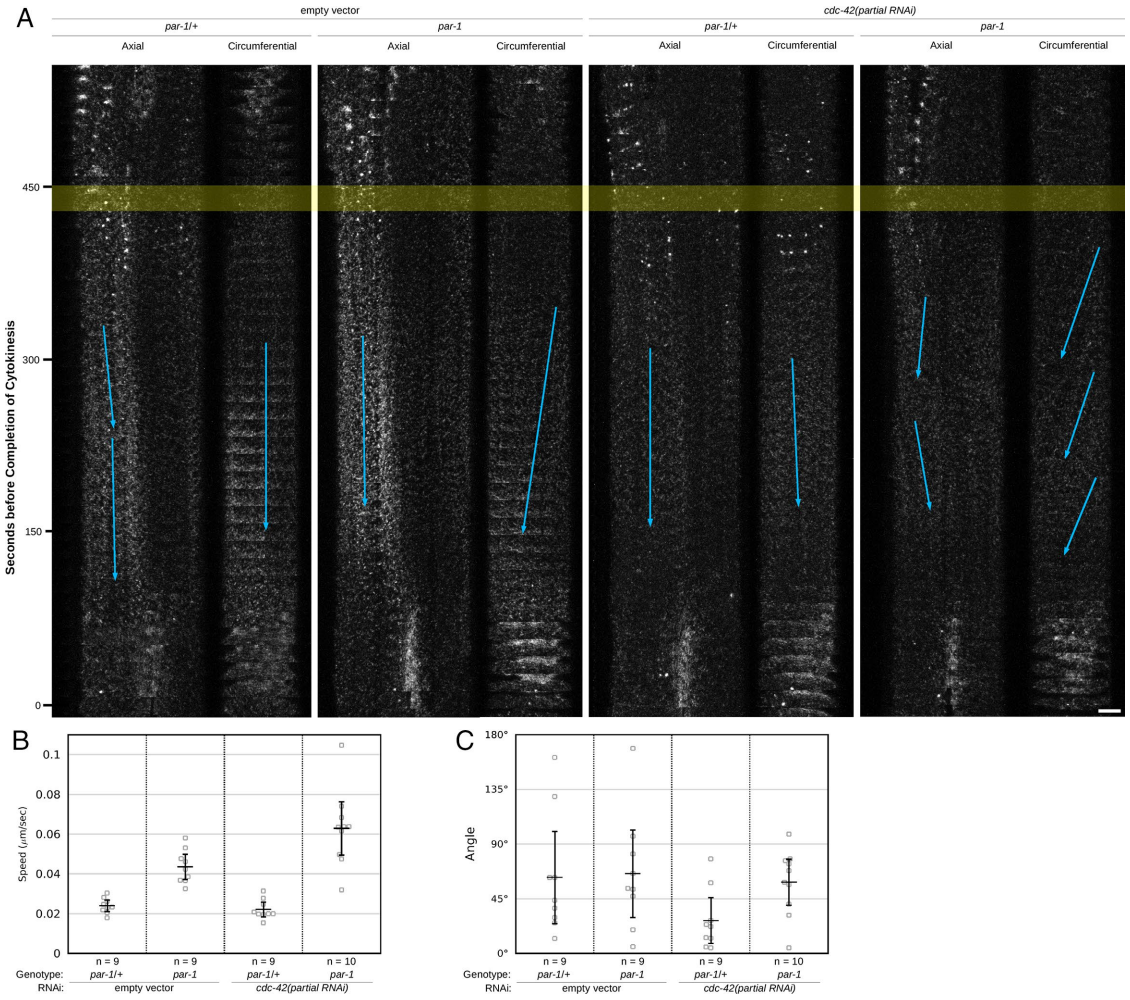

FIGURE 8: CDC-42 inhibits NMY-2::GFP cortical movement in the absence of PAR-1. (A) Movement of cortical NMY-2::GFP in *par-1* or *par-1*/+ embryos treated with empty vector or *cdc-42* partial RNAi. Kymographs are constructed as in Figure 5. (B, C) Average speed (B) and direction (C) of movement of NMY-2::GFP foci in *par-1* mutant and *par-1*/+ balanced embryos treated with empty vector or *cdc-42* partial RNAi. Graphs are constructed as in Figure 5.

required for high levels of CDC-42 activity, and in the absence of PAR-6, the biosensor used previously may be unable to detect residual CDC-42 activity.

Our *par* phenotypes place several requirements on unknown regulatory intermediates between PAR proteins and NMY-2. It is not sufficient for PAR-3 and PAR-6 to simply promote an NMY-2 activator in the anterior because this would not explain the observed increase in posterior NMY-2 association in *par-3* and *par-6* embryos. PAR-3 and PAR-6 repression of an NMY-2 inhibitor in the anterior is not sufficient, for the same reason. One possibility is that the hypothetical intermediate NMY-2 regulator is present in limiting amounts. The elevated NMY-2 we see in *par-2* embryos precludes this possibility for a hypothetical NMY-2 activator. A second possibility is that there is both an NMY-2 activator and inhibitor and that *par-3* or *par-6* mutation causes these two to mix across the cortex, resulting in an intermediate level of cortical NMY-2.

The stabilizing influence of PAR-3 on the polarized cortex

Our observed *par-3* phenotypes provide insight into PAR-3's contribution to maintenance of polarity when knowledge of these phenotypes is combined with knowledge of PAR-3's molecular function. PAR-3 functions as a structural protein, oligomerizing with itself and binding to PAR-6 and PKC-3 (Tabuse, Izumi, *et al.*, 1998; Benton and St. Johnson, 2003). We hypothesize that it has a stabilizing effect on the anterior domain, providing a relatively static substrate to which other anterior proteins are recruited. Research shows that PAR-2 and PAR-6 both have the ability to freely diffuse across the domain boundary (Goehring *et al.*, 2011). In addition, there is a population of PAR-6 that does not freely diffuse, and this second population may be the one that is bound to PAR-3 (Beers and Kemphues, 2006; Robin *et al.*, 2014). To our knowledge, the diffusibility of PAR-3 has not been measured. In the absence of PAR-3, we hypothesize that CDC-42–associated PAR-6 generates the moving NMY-2 patch and is able to freely migrate across the cortex. In the presence of PAR-3, a portion of PAR-6 is held in place by PAR-3 oligomers, and, as a result, PAR-3 prevents the anterior domain from shifting.

The role of PAR-2 in inhibiting NMY-2 association

According to our results, the role of PAR-2 with respect to NMY-2 localization is to inhibit PAR-A, preventing PAR-A, and by extension NMY-2, from associating with the posterior cortex. We do not believe that PAR-2 has the ability to directly inhibit NMY-2 association. In the absence of PAR-A, PAR-2 becomes ubiquitously distributed across the cortex (Boyd *et al.*, 1996; Cuenca *et al.*, 2003). If PAR-2 had a

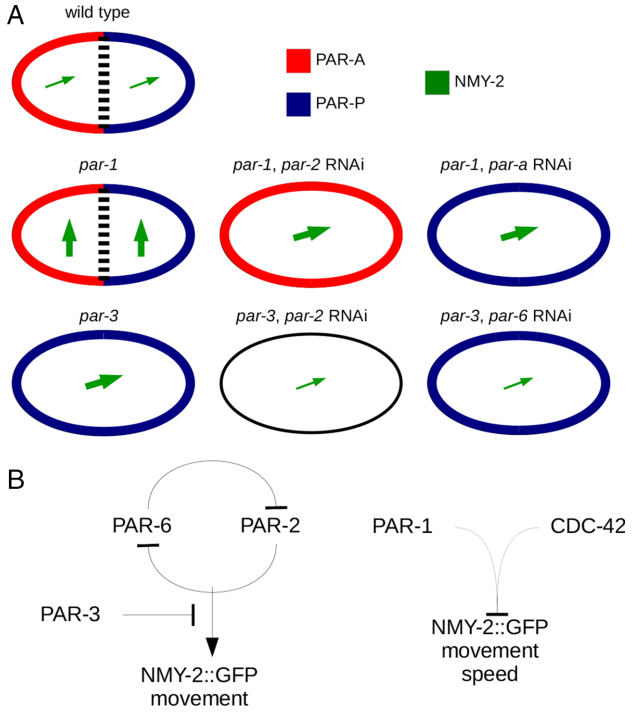

FIGURE 9: PAR proteins regulate NMY-2 movement. (A) Observed NMY-2::GFP movement under different combinations of *par* mutation and RNAi. PAR-A and PAR-P proteins are represented as in Figure 1A. NMY-2 is represented as an arrow, the weight of which indicates movement speed and the direction of which indicates movement direction. (B) Cartoon of observed genetic interactions. Pointed arrows indicate positive interactions, and blunt arrows indicate negative interactions.

direct inhibitory effect, we would expect an increase in NMY-2 association in doubly deficient embryos in the absence of PAR-3 or PAR-6, although perhaps not to wild-type anterior levels. Technically, however, our experiment cannot differentiate between the explanation presented here and the situation in which, added to this, there is also a posterior NMY-2–inhibiting factor that directly requires PAR-2 but is inhibited by PAR-3 and PAR-6.

Previous results for epistasis between *par-2* and *par-3* are mixed in their agreement with ours: Zonies *et al.* (2010) also found that doubly deficient embryos had uniformly moderate levels of cortical NMY-2, whereas Munro *et al.* (2004) found uniformly high levels of cortical NMY-2. Previous results for epistasis between *par-2* and *par-6* do not agree with ours: Beatty *et al.* (2013) found uniformly high levels of cortical NMY-2 in double-mutant embryos. On the other hand, Sailer *et al.* (2015) examined the CDC-42–inactivating protein CHIN-1 instead of NMY-2 and found that both *par-3* and *par-6* were epistatic to *par-2*. All characterizations of NMY-2 levels use the same *nmy-2::gfp* transgene (Nance *et al.*, 2003), and so the discrepancies are not due to different transgene expression levels. It is possible that the different use of RNAi and *par* mutant alleles is responsible for the observed differences in regulation. It is also possible that the results of Beatty *et al.* (2013) are confounded by their use of *unc-45*ts as a *par-2* marker allele; *unc-45* itself has been shown to affect NMY-2 cortical association in the zygote (Kachur *et al.*, 2004, 2008). In the future, we will assay other components of the CDC-42 pathway in *par* mutant embryos so that the full nuances of the system can be uncovered and anomalous results can be more easily identified.

par-1 prevents NMY-2 movement during maintenance phase

Here we explicitly studied the role of PAR-1, a historically overlooked protein, in regulating NMY-2. Many studies focus attention on PAR-2 because it is required for PAR-1 to associate with the cortex when PAR-3 is present, and *par-1* mutations do not have significant maintenance-phase phenotypes (Etemad-Moghadam *et al.*, 1995; Boyd *et al.*, 1996; Motegi *et al.*, 2011). Of interest, however, there have been hints that PAR-1 has a larger role to play, specifically involving the actin-myosin cortex. NMY-2 was first identified as a protein that physically interacts with PAR-1 (Guo and Kemphues, 1996). In addition, an actin filament reporter reveals a reduced anterior domain at the end of establishment phase under *par-1* RNAi (Velarde *et al.*, 2007). Our discovery of ectopic NMY-2 movement contributes another instance of PAR-1 interacting with the actin-myosin cortex.

The cause of ectopic NMY-2 movement in *par-1* embryos is still unknown. Several potential causes have been ruled out by this study: CDC-42 activity, asymmetric NMY-2 pulling forces, and PAR-A/PAR-P dynamic interactions. Astral microtubules have been shown to be necessary for stability of the A/P domain boundary (Ai *et al.*, 2011). During the maintenance phase, the mitotic spindle forms and undergoes stereotypical movements (Albertson, 1984). Perhaps astral microtubules or cortically associated microtubule motors exert rotational forces on the cortex as they move the pronuclear complex and mitotic spindle. This hypothesis is supported by the fact that PAR-1 homologues are known as regulators of microtubule dynamics in other organisms (Drewes *et al.*, 1997; Doerflinger *et al.*, 2003; Sapir *et al.*, 2008a,b; Hayashi *et al.*, 2011; Nishimura *et al.*, 2012). This hypothesis would also suggest an interpretation of our observation that RNAi against *par-2*, *par-3*, and *par-6* is able to alter the direction of cortical movement because mutating these *par*s produces defects in pronuclear migration and spindle positioning (Kemphues *et al.*, 1988; Watts *et al.*, 1996; Sönnichsen *et al.*, 2005). We hypothesize that PAR-1, in cooperation with CDC-42, stiffens the actin-myosin cortex so that it is capable of resisting the forces produced by pronuclear complex and spindle dynamics. Important questions for further characterization of this process include determining the relevant targets of PAR-1 phosphorylation and the forces that drive NMY-2 movement.

MATERIALS AND METHODS

Strain maintenance and genetics

Supplemental Table S1 lists strains used in this study. Strains were maintained as previously described (Brenner, 1974). All strains were grown at 20°C except EU822 and ATD2, which were grown at 15°C. The *par-2(or373*ts*)* phenotype was induced at the restrictive temperature of 25°C for >24 h. For crosses, JJ1473 males were generated by heat shock of L4 hermaphrodites at 30°C for 8 h or 31.5°C for 6 h. All strains generated in this study have been deposited at the *Caenorhabditis* Genetics Center (https://cgc.umn.edu).

RNA interference

RNAi was administered by feeding (Kamath *et al.*, 2001). RNAi plasmids were obtained from the Ahringer RNAi Library (Kamath, Fraser *et al.*, 2003), sequenced, and retransformed into HT115 *Escherichia coli*. HT115 *E. coli* cultures carrying an RNAi plasmid were grown overnight at 37°C in Lysogeny broth–Miller (BP1426-2; Fisher Scientific) plus 50 μg/ml carbenicillin. RNAi cultures were seeded on nematode growth medium–agar plates supplemented with 25 μg/ml carbenicillin and 1 mM isopropyl-β-D-thiogalactoside and grown overnight at 37°C. For complete RNAi, 3-d-old worms were picked to RNAi plates the next morning and incubated at

25°C for >24 h. For partial RNAi, 4-d-old worms were picked to RNAi plates the next morning and incubated at 25°C for 7–10 h. Empty vector controls were performed using the L4440 (also known as pPD129.36) feeding vector (Timmons and Fire, 1998). Strength of *par* RNAi was ensured by the presence of published *par* division phenotypes: symmetrical first division in *par-2*, *par-3*, and *par-6* and synchronous second division in *par-1* (Kemphues *et al.*, 1988; Watts *et al.*, 1996).

Confocal microscopy

Embryos were dissected from hermaphrodites on a coverslip into Egg Salts (118 mM NaCl, 40 mM KCl, 3.4 mM $CaCl_2$, 3.4 mM $MgCl_2$), inverted onto a 1% agar pad prepared with Egg Salts, and sealed with Petrolatum. Images were taken of the face of the embryo cortex nearer to the coverslip every 15 s at ambient temperature. Confocal fluorescence microscopy was performed on two different systems. Except in Supplemental Figure S2, images were taken using an LSM700 scanning confocal system (Zeiss) attached to an Axio Observer.Z1 inverted microscope (Zeiss) equipped with a 63×/1.4 numerical aperture (NA) Plan Achromat oil immersion objective (Zeiss) and a Definite Focus focal drift correction system (Zeiss). Acquisition was controlled by ZEN Black software (Zeiss). Illumination was performed with a 488-nm solid-state diode laser, and images were collected with the LSM700 built-in photomultiplier tube. Four *z*-sections of width 0.70 µm were spaced 0.35 µm apart. Embryos were oriented with the anterior pole to the left. Images in Supplemental Figure S2 were taken using an UltraVIEW Vox CSUX1 spinning-disk confocal system (PerkinElmer) attached to a Ti-E inverted microscope (Nikon) equipped with a 100×/1.4NA Plan Apo oil immersion objective (Nikon) and a Perfect Focus focal drift correction system (PerkinElmer). Acquisition was controlled by Volocity software (PerkinElmer). Illumination was performed with a 488-nm solid-state laser, and images were collected with a back-thinned electron-multiplying charge-coupled device camera (C9100-13; Hamamatsu Photonics). Six *z*-sections of width 0.50 µm were spaced 0.25 µm apart.

Image analysis

Image sequences were imported into Fiji (Schindelin *et al.*, 2012) or MATLAB (www.mathworks.com/products/matlab) using Bio-Formats (www.openmicroscopy.org/site/support/bio-formats5.1/about/). *Z*-stacks were flattened by maximum intensity projection. Images taken with the spinning-disk microscope were rotated in Fiji so that the embryo's anterior pole was to the left. Videos were scaled and encoded for publication using FFmpeg (www.ffmpeg.org). Average pixel intensity was determined in specific regions of the visible cortex as described in figure captions. Pixel intensities were normalized to average anterior fluorescence of balanced and empty vector (where appropriate) embryos imaged alongside the experimental embryos. When warranted, the maximum grayscale value of displayed images is normalized in the same way.

Most measurements of NMY-2::GFP foci movement were performed on kymographs constructed from the aforementioned image sequences described. From each image sequence, two kymographs were constructed from perpendicular sections: parallel to the A/P axis (axial) and perpendicular to the A/P axis (circumferential; Figure 5 A). Sections were 5 µm thick and 15 s apart. Foci were measured by tracing their movement down the kymographs. The slope of these traces at each time point along the kymographs yielded foci velocities in the axial and circumferential dimensions; these velocities were then combined to obtain speed and angle parameters for foci movement at each time point. Direction of movement toward the posterior pole was defined as 0° and toward the anterior pole as 180°. Because *C. elegans* zygotes have no dorsal/ventral markers, measurements from each embryo with a downward mean angle (>180°) were reflected across the A/P axis so that all mean angles were in the interval [0°, 180°].

Measurement of NMY-2::GFP foci movement in Supplemental Figure S1 was performed as described, except that anterior and posterior portions of each embryo were cropped from the image sequence and measured independently. Measurement of NMY-2::GFP foci movement in Supplemental Figure S4 via the tiled method was performed as described, except that, instead of single axial and circumferential kymographs, multiple kymographs in each direction were tiled across the embryo image.

Statistical methods

The 95% confidence intervals (CIs) of the mean indicate that identically performed experiments will contain the true mean within their CIs 95% of the time (Krzywinski and Altman, 2013). They were calculated in MATLAB using the formula $CI = \pm t(s/\sqrt{n})$, where s is sample SD, n is number of samples, and t is the critical t value at $1 - \alpha = 0.95$ and degrees of freedom $n - 1$.

ACKNOWLEDGMENTS

We thank Helen Chamberlin for the L4440 (pPD129.36) plasmid and clones from the Ahringer RNAi library, as well as members of the Chamberlin and Dawes labs for helpful suggestions, reagents, and technical assistance. We thank Robin Wharton, Helen Chamberlin, and Jian-Qiu Wu for valuable discussions and critical reading of the manuscript. Some strains used in this study were provided by the *Caenorhabditis* Genetics Center (Supplemental Table S1), which is funded by the National Institutes of Health Office of Research Infrastructure Programs (P40 OD010440). This study was funded by National Science Foundation/National Institutes of Health Grant DMS/NIGMS-1361231 to A.T.D.

REFERENCES

Boldface names denote co–first authors.

Aceto D, Beers M, Kemphues KJ (2006). Interaction of PAR-6 with CDC-42 is required for maintenance but not establishment of PAR asymmetry in *C. elegans*. Dev Biol 299, 386–397.

Ai E, Poole DS, Skop AR (2011). Long astral microtubules and RACK-1 stabilize polarity domains during maintenance phase in *Caenorhabditis elegans* embryos. PLoS One 6, e19020.

Albertson DG (1984). Formation of the first cleavage spindle in nematode embryos. Dev Biol 101, 61–72.

Beatty A, Morton DG, Kemphues K (2013). PAR-2, LGL-1 and the CDC-42 GAP CHIN-1 act in distinct pathways to maintain polarity in the *C. elegans* embryo. Development 140, 2005–2014.

Beers M, Kemphues K (2006). Depletion of the co-chaperone CDC-37 reveals two modes of PAR-6 cortical association in *C. elegans* embryos. Development 133, 3745–3754.

Benton R, St. Johnson D (2003). A conserved oligomerization domain in *Drosophila* Bazooka/PAR-3 is important for apical localization and epithelial polarity. Curr Biol 13, 1130–1134.

Boyd L, Guo S, Levitan D, Stinchcomb DT, Kemphues KJ (1996). PAR-2 is asymmetrically distributed and promotes association of P granules and PAR-1 with the cortex in *C. elegans* embryos. Development 122, 3075–3084.

Brenner S (1974). The genetics of *Caenorhabditis elegans*. Genetics 77, 71–94.

Cheng NN, Kirby CM, Kemphues KJ (1995). Control of cleavage spindle orientation in *Caenorhabditis elegans*: the role of the genes *par-2* and *par-3*. Genetics 139, 549–559.

Cuenca AA, Schetter A, Aceto D, Kemphues K, Seydoux G (2003). Polarization of the *C. elegans* zygote proceeds via distinct establishment and maintenance phases. Development 130, 1255–1265.

Doerflinger H, Benton R, Shulman JM, St Johnson D (2003). The role of PAR-1 in regulating the polarized microtubule cytoskeleton in the *Drosophila* follicular epithelium. Development 130, 3965–3975.
Drewes G, Ebneth A, Preuss U, Mandelkow EM, Mandelkow E (1997). MARK, a novel family of protein kinases that phosphorylate microtubule-associated proteins and trigger microtubule disruption. Cell 89, 297–308.
Etemad-Moghadam B, Guo S, Kemphues KJ (1995). Asymmetrically distributed PAR-3 protein contributes to cell polarity and spindle alignment in early *C. elegans* embryos. Cell 83, 743–752.
Goehring NW, Hoege C, Grill SW, Hyman AA (2011). PAR proteins diffuse freely across the anterior–posterior boundary in polarized *C. elegans* embryos. J Cell Biol 193, 583–594.
Gotta M, Abraham MC, Ahringer J (2001). CDC-42 controls early cell polarity and spindle orientation in *C. elegans*. Curr Biol 11, 482–488.
Griffin EE, Odde DJ, Seydoux G (2011). Regulation of the MEX-5 gradient by a spatially segregated kinase/phosphatase cycle. Cell 146, 955–968.
Guo S, Kemphues KJ (1995). *par-1*, a gene required for establishing polarity in *C. elegans* embryos, encodes a putative Ser/Thr kinase that is asymmetrically distributed. Cell 81, 611–620.
Guo S, Kemphues KJ (1996). A non-muscle myosin required for embryonic polarity in *Caenorhabditis elegans*. Nature 382, 455–458.
Hao Y, Boyd L, Seydoux G (2006). Stabilization of cell polarity by the *C. elegans* RING protein PAR-2. Dev Cell 10, 199–208.
Harris KP, Tepass U (2010). Cdc42 and vesicle trafficking in polarized cells. Traffic 11, 1272–1279.
Hayashi K, Suzuki A, Hirai S, Kurihara Y, Hoogenraad CC, Ohno S (2011). Maintenance of dentritic spine morphology by partitioning-defective 1b through regulation of microtubule growth. J Neurosci 31, 12094–12103.
Hung TJ, Kemphues KJ (1999). PAR-6 is a conserved PDZ domain-containing protein that colocalizes with PAR-3 in *Caenorhabditis elegans* embryos. Development 126, 127–135.
Hurd DD, Kemphues KJ (2003). PAR-1 is required for morphogenesis of the *Caenorhabditis elegans* vulva. Dev Biol 253, 54–65.
Kachur T, Ao W, Berger J, Pilgrim D (2004). Maternal UNC-45 is involved in cytokinesis and colocalizes with non-muscle myosin in the early *Caenorhabditis elegans* embryo. J Cell Sci 117, 5313–5321.
Kachur TM, Audhya A, Pilgrim DB (2008). UNC-45 is required for NMY-2 contractile function in early embryonic polarity establishment and germline cellularization in *C. elegans*. Dev Biol 314, 287–299.
Kamath RS, Martinez-Campos M, Zipperlen P, Fraser AG, Ahringer J (2001). Effectiveness of specific RNA-mediated interference through ingested double-stranded RNA in *Caenorhabditis elegans*. Genome Biol 2, research0002.
Kamath RS, Fraser AG, Dong Y, Poulin G, Durbin R, Gotta M, Kanapin A, Le Bot N, Moreno S, Sohrmann M, *et al*. (2003). Systematic functional analysis of the *Caenorhabditis elegans* genome using RNAi. Nature 421, 231–237.
Kay AJ, Hunter CP (2001). CDC-42 regulates PAR protein localization and function to control cellular and embryonic polarity in *C. elegans*. Curr Biol 11, 474–481.
Kemphues KJ, Priess JR, Morton DG, Cheng N (1988). Identification of genes required for cytoplasmic localization in early *C. elegans* embryos. Cell 52, 311–320.
Krzywinski M, Altman N (2013). Points of significance: error bars. Nat Methods 10, 921–922.
Kumfer KT, Cook SJ, Squirrell JM, Eliceiri KW, Peel N, O'Connell KF, White JG (2010). CGEF-1 and CHIN-1 regulate CDC-42 activity during asymmetric division in the *Caenorhabditis elegans* embryo. Mol Biol Cell 21, 266–277.
Levitan DJ, Boyd L, Mello CC, Kemphues KJ, Stinchcomb DT (1994). *par-2*, a gene required for blastomere asymmetry in *Caenorhabditis elegans*, encodes zinc-finger and ATP-binding motifs. Proc Natl Acad Sci USA 91, 6108–6112.
Liu J, Maduzia LL, Shirayama M, Mello CC (2010). NMY-2 maintains cellular asymmetry and cell boundaries, and promotes a SRC-dependent asymmetric cell division. Dev Biol 339, 366–373.
Motegi F, Sugimoto A (2006). Sequential functioning of the ECT-2 RhoGEF, RHO-1 and CDC-42 establishes cell polarity in *Caenorhabditis elegans* embryos. Nature 8, 978–985.
Motegi F, Zonies S, Hao Y, Cuenca AA, Griffin E, Seydoux G (2011). Microtubules induce self-organization of polarized PAR domains in *Caenorhabditis elegans* zygotes. Nat Cell Biol 13, 1361–1367.
Munro E, Nance J, Priess JR (2004). Cortical flows powered by asymmetrical contraction transport PAR proteins to establish and maintain anterior-posterior polarity in the early *C. elegans* embryo. Dev Cell 7, 413–424.
Nance J, Munro EM, Priess JR (2003). *C. elegans* PAR-3 and PAR-6 are required for apicobasal asymmetries with cell adhesion and gastrulation. Development 130, 5339–5350.
Nishimura Y, Applegate K, Davidson MW, Danuser G, Waterman CM (2012). Automated screening of microtubule growth dynamics identifies MARK2 as a regulator of leading edge microtubules downstream of Rac1 in migrating cells. PLoS One 7, e41413.
O'Rourke SM, Carter C, Carter L, Christensen SN, Jones MP, Nash B, Price MH, Turnbull DW, Garner AR, Hamill DR, *et al*. (2011). A survey of new temperature-sensitive, embryonic-lethal mutations in *C. elegans*: 24 alleles of thirteen genes. PLoS One 6, e16644.
Ou G, Stuurman N, D'Ambrosio M, Vale RD (2010). Polarized myosin produces unequal-sized daughters during asymmetric cell division. Science 330, 677–680.
Robin FB, McFadden WM, Yao B, Munro EM (2014). Single-molecule analysis of cell surface dynamics in *Caenorhabditis elegans* embryos. Nat Methods 11, 677–682.
Sailer A, Anneken A, Li Y, Lee S, Munro E (2015). Dynamic opposition of clustered proteins stabilizes cortical polarity in the *C. elegans* zygote. Dev Cell 35, 131–142.
Sapir T, Sapoznik S, Levy T, Finkelshtein D, Shmueli A, Timm T, Mandelkow EM, Reiner O (2008a). Accurate balance of the polarity kinase MARK2/Par-1 is required for proper cortical neuronal migration. J Neurosci 28, 5710–5720.
Sapir T, Shmueli A, Levy T, Timm T, Elbaum M, Mandelkow EM, Reiner O (2008b). Antagonistic effects of doublecortin and MARK-2/Par-1 in the developing cerebral cortex. J Neurosci 28, 13008–13013.
Schindelin J, Arganda-Carreras I, Frise E, Kaynig V, Longair M, Pietzsch T, Preibisch S, Rueden C, Saalfeld S, Schmid B, *et al*. (2012). Fiji: an open-source platform for biological-image analysis. Nat Methods 9, 676–682.
Schonegg S, Hyman AA (2006). CDC-42 and RHO-1 coordinate acto-myosin contractility and PAR protein localization during polarity establishment in *C. elegans* embryos. Development 133, 3507–3516.
Schubert CM, Lin R, de Vries CJ, Plasterk RHA, Priess JR (2000). MEX-5 and MEX-6 function to establish soma/germline asymmetry in early *C. elegans* embryos. Mol Cell 5, 671–682.
Sönnichsen B, Koski LB, Walsh A, Marschall P, Neumann B, Brehm M, Alleaume AM, Artelt J, Bettencourt P, Cassin E, *et al*. (2005). Full-genome RNAi profiling of early embryogenesis in *Caenorhabditis elegans*. Nature 434, 462–469.
Tabuse Y, Izumi Y, Piano F, Kemphues KJ, Miwa J, Ohno S (1998). Atypical protein kinase C cooperates with PAR-3 to establish embryonic polarity in *Caenorhabditis elegans*. Development 125, 3607–3614.
Tenlen JR, Molk JN, London N, Page BD, Priess JR (2008). MEX-5 asymmetry in one-cell *C. elegans* embryos requires PAR-4- and PAR-1-dependent phosphorylation. Development 135, 3665–3675.
Timmons L, Fire A (1998). Specific interference by ingested dsRNA. Nature 395, 854.
Velarde N, Gunsalus KC, Piano F (2007). Diverse roles of actin in *C. elegans* early embryogenesis. BMC Dev Biol 7, 142.
Watts JL, Etemad-Moghadam B, Guo S, Boyd L, Draper BW, Mello CC, Priess JR, Kemphues KJ (1996). *par-6*, a gene involved in the establishment of asymmetry in early *C. elegans* embryos, mediates the asymmetric localization of PAR-3. Development 122, 3133–3140.
Willis JH, Munro E, Lyczak R, Bowerman B (2006). Conditional dominant mutations in the *Caenorhabditis elegans* gene *act-2* identify cytoplasmic and muscle roles for a redundant actin isoform. Mol Biol Cell 17, 1051–1064.
Zonies S, Motegi F, Hao Y, Seydoux G (2010). Symmetry breaking and polarization of the *C. elegans* zygote by the polarity protein PAR-2. Development 137, 1669–1677.